

Experimental Studies on Structural, Electrical and Thermal Properties of $\text{Bi}_{0.7}\text{Sm}_{0.3}\text{FeO}_3$ Ceramic

Vikash Kumar Jha^{1,a)} and M. Roy^{1,b)*}

Department of Physics, Mohanlal Sukhadia University, Udaipur-313001, Rajasthan, India

^{b)*}Corresponding author: mroy1959@yahoo.co.in

^{a)}vkjha1988@yahoo.com

Abstract: Multiferroic $\text{Bi}_{0.7}\text{Sm}_{0.3}\text{FeO}_3$ ceramic has been prepared by standard high temperature solid state reaction method using high purity oxides. The formation of compound and its structural parameters were investigated by X-ray diffraction followed by Rietveld refinement using centrosymmetric space group Pbnm. The dielectric constant and dissipation factor as a function of frequency and temperature has been measured. The ac conductivity has been measured from temperature dependant dissipation factor curve. The dc conductivity of the compound increases with increase of temperature. The activation energy has been calculated from the slope of the dc conductivity curve by using Arrhenius relation $\sigma = \sigma_0 \exp(-E_a/kT)$ and the obtained value is 0.25 eV. The endothermic sluggish peak around 1020 K along with small weight loss (1.24% of initial weight) from room temperature (RT) to 1173 K confirms that the prepared ceramic is thermally stable at high temperature.

INTRODUCTION

Researchers have been involve to study the preparation and characteristics of multiferroic materials from some decades due to its unique physical phenomena i.e. ferroelectricity, ferromagnetism and ferroelasticity produced in same phase at RT [1-2]. Bismuth Ferrite, (BiFeO_3), generally known as BFO, is such a type of multiferroic ceramic which has been widely interesting material for scientific community to its unique physical characteristics which has been applied in various device applications (memory storage, sensors, capacitors, solar energy cells etc.) [3-5]. BFO shows ferroelectric Curie temperature (T_C) at 1083K and antiferromagnetic Neel temperature (T_N) at 643 K [1]. The structure of the compound has been observed as rhombohedral with space symmetry R3c but in some research papers, triclinic structure of BFO has also been reported [1, 6]. BFO contains high leakage current phenomena along with high coercive fields as well as electromagnetic coefficients are much smaller than the conventional lead based compositions, which are main drawbacks of this compound [7]. So many studies have been reported to remove these drawbacks with substitution of rare earth oxides in A-site and Zn, Mn, Co, Sc etc. in B-site of BFO but no any report is available to claim the complete removal of these drawbacks from BiFeO_3 [6-8]. Yao et al. reported that the oxygen vacancies were responsible for electrical conduction and calculated activation energy under dc field has been found to be 0.7 eV via 8% Sm doping in A-site of BFO [8]. Also, Palaimiene et al. reported that the activation energy was 0.54 eV by 20% Sm doping and observed that the dielectric properties of Sm doped BFO ceramics were governed by electrical conductivity and Maxwell-Wagner relaxation [9]. In this report, we present the study of structural, electrical and thermal properties via 30% Sm doping in A-site of BFO, to understand the mechanism and characteristics of this compound in different device applications.

EXPERIMENTAL

The polycrystalline $\text{Bi}_{0.7}\text{Sm}_{0.3}\text{FeO}_3$ ceramic sample has been prepared by the conventional high-temperature solid-state reaction method using high purity analytical grade oxides. The stoichiometric amount of Bi_2O_3 , Fe_2O_3 and Sm_2O_3 were mixed and grounded manually in presence of acetone [$(\text{CH}_3)_2\text{CO}$] up to 6-10 hours. These grounded mixtures were calcined for 12 hours in a muffle furnace at 773-1073 K. Pellet has been made via compression of 5

tons/cm² using a hydraulic press. Then this pellet was sintered at 1148 K up to 10 minutes in the same furnace. The structure of the prepared sample was characterized by Rigaku Mini Flex Ultima-IV X-ray diffractometer in the angle 2θ from 20° to 90° range with a rate of 2°/minute and a step size 0.02°. The dielectric constant (ε') and dissipation factor (ε'') were measured as a function of frequency from 1 kHz to 5MHz and temperature 303K to 623K using Hioki 3532-50 LCR Hi tester. The ac conductivity of the compound was calculated from dissipation factor curve using equation $\sigma_{ac} = \epsilon_0 \epsilon_r \omega \tan \delta$ -- (1), where permittivity of free space is ϵ_0 , relative permittivity is ϵ_r , angular frequency is ω and dielectric loss is $\tan \delta$. The dc conductivity measurement was carried out by two probe method using lab made set up from room-temperature to 623K and the activation energy of the compound has been calculated from Arrhenius relation $\sigma = \sigma_0 \exp(-E_a/kT)$ -- (2). The heat flow and weight loss of the compound as a function of temperature (303-1173) K were carried out with a heating rate of 30K/minute in the inert atmosphere (N₂) using DTA/TGA Perkin Elmer thermal analyzer (STA-6000).

RESULTS AND DISCUSSION

Structural analysis

The Rietveld refinement of X-ray diffraction pattern of Bi_{0.7}Sm_{0.3}FeO₃ ceramic has been done using Fullprof program and is shown in Figure 1. The Orthorhombic structure with space group Pbnm confirms that the formation of this compound is in single phase and free from impurity peaks. Usually, BFO shows the rhombohedral structure with space group R3c [1]. The calculated XRD pattern of the sample coincides well with the observed XRD pattern with small R-values and these values are listed in Table 1. These small R-values confirm that the formation of the Sm-doped compound during the high-temperature solid-state reaction between Bi₂O₃, Sm₂O₃, and Fe₂O₃ is completed under the controlled sintering conditions. The Crystallite size (D) of the compound is 0.04μm, which has been calculated using the Scherer formula, $D = \frac{k\lambda}{\beta \cos \theta}$ -- (3), where k is Scherer constant having value 0.94 and β is the full width at half maximum (FWHM) [10]. The dislocation density (δ) of the compound has been calculated using the Williamson–Smallman relation $\delta = \frac{1}{D^2}$ -- (4) and the calculated value of δ is 132.15(μm)⁻². The strain (ε) of the compound has been calculated using the equation $\epsilon = \frac{\beta}{4 \tan \theta}$ -- (5) and the calculated value of ε is 0.05922. Also, the number of crystallites per unit area (N) of the compound has been calculated using the relation $N = \frac{t}{D^3}$ -- (6), where t is the thickness of the sample and the calculated value of N is 400827(μm)⁻².

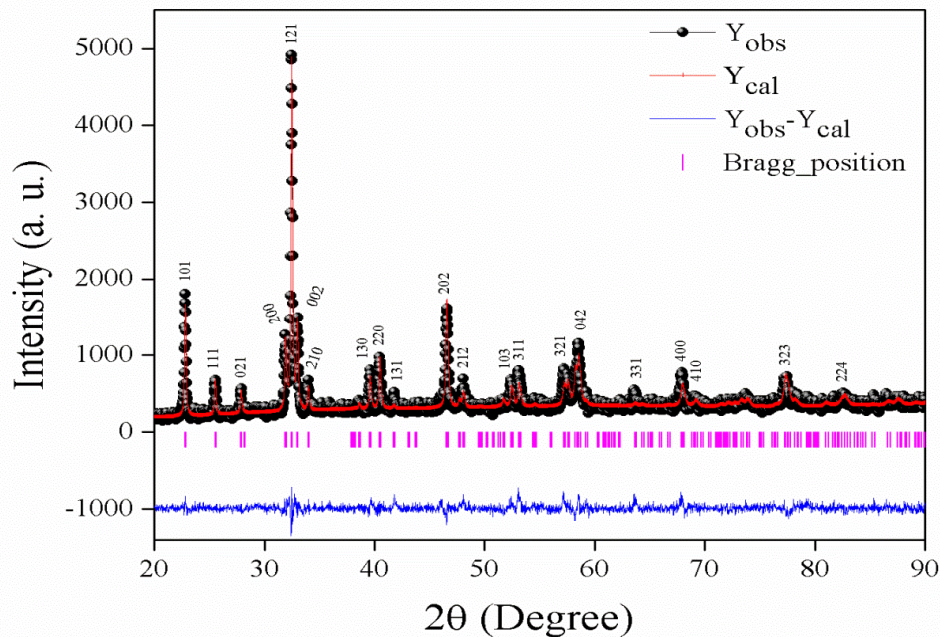


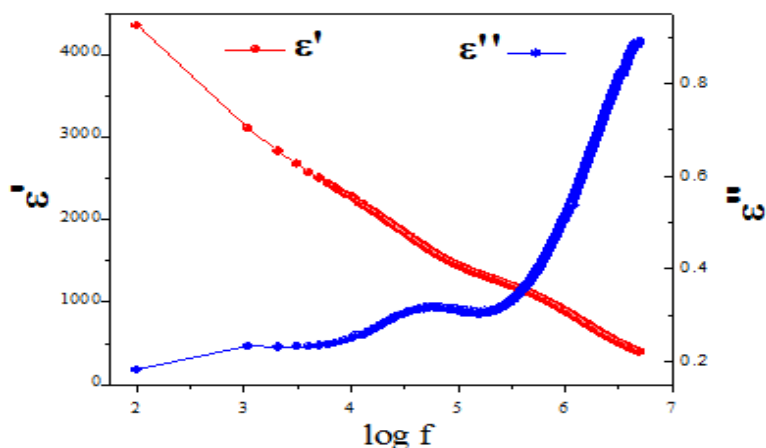
FIGURE 1. Rietveld refined profile of Bi_{0.7}Sm_{0.3}FeO₃

TABLE 1: Rietveld refinement parameters

a (Å)	5.6056
b (Å)	7.7948
c (Å)	5.4289
Unit cell volume (Å) ³	237.214
Density (g/cm ³)	21.982
R _{Bragg}	9.74
R _f	11.1
R _p	19.9
R _{wp}	11.3
R _e	7.6
χ^2	3.5
GOF	2.1

Electrical properties

The variation of dielectric constant (ϵ') and dissipation factor (ϵ'') has been plotted as a function of frequency and is shown in Figure 2. It is observed that ϵ' is a strong function of frequency which decreases continuously with the increase of frequency and reverse trend is obtained for the ϵ'' . This decreasing trend of ϵ' with respect to frequency is due to the inability of the electric dipoles to switch with the applied electric field at higher frequencies [11]. Due to the presence of all types of polarizations which align themselves in one direction with the applied field hence the ϵ' shows the high value at low frequency region. But dipoles cannot synchronize with the applied field and frequency hence; the contribution of polarization reduces and appears to merge into a single line which results the small value of dielectric constant at high-frequency region [12]. The increase in ϵ'' with frequency (inset of Figure 2) is due to the higher conductivity causing higher leakage current [10]. As a matter of fact, applied electric field, temperature, doping and structural defects are the factors which influence dielectric properties. At 1MHz, a small hump is observed which emphasize the decreasing nature of dielectric loss in high frequency range.

**FIGURE 2.** ϵ' and ϵ'' vs. frequency curve at RT

The dielectric constant (ϵ') vs. temperature curve at different frequencies of 10 kHz, 100 kHz and 1 MHz has been plotted in Figure 3. The 100 kHz and 1 MHz frequency curves show almost temperature independent behavior up to 350K and then increases up to the measured temperature range while ϵ' is increasing with temperature for 10 kHz frequency due to the smaller crystalline size of the compound which is the characteristic of a good dielectric material. The reason behind that such an increase may be the thermally activated hopping between Fe^{2+} and Fe^{3+} which leads to local displacement of hopping charges in the direction of electric field and thus results in the

polarization and hence the increase in dielectric constant [13]. The ϵ' decreases with increasing frequency from 10 kHz to 1 MHz.

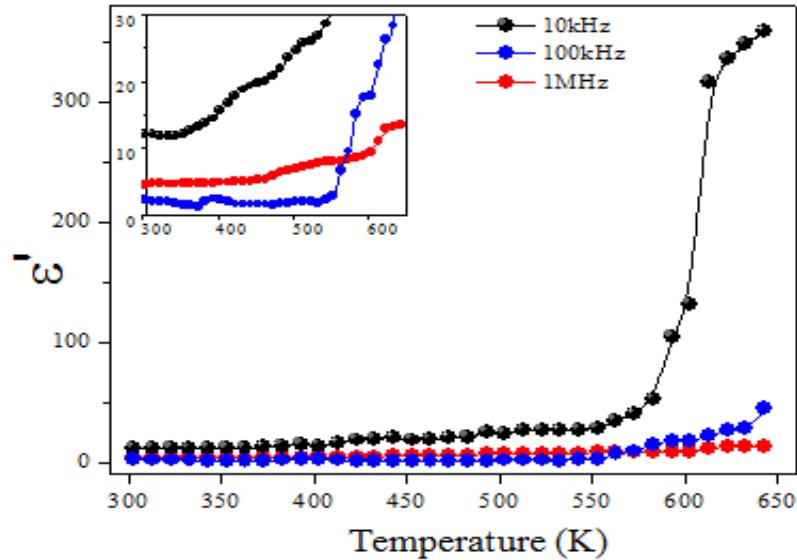


FIGURE 3. ϵ' vs. temperature curve

The dissipation factor (ϵ'') vs. temperature curve at 10 kHz, 100 kHz and 1 MHz frequencies are plotted in Figure 4. The ϵ'' shows the almost same trend as ϵ' but very small in magnitude. From 500 K, ϵ'' increases with temperature, indicates that it is strongly temperature dependent in the high-temperature region.

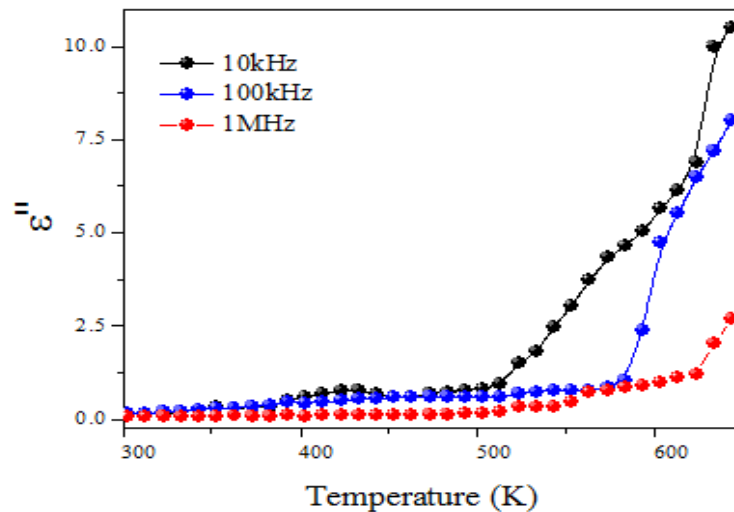


FIGURE 4. ϵ'' vs. temperature curve.

The ac conductivity increases with temperature for different frequencies 10 kHz, 100 kHz and 1 MHz and is shown in Figure 5. For 10 kHz, there is a small hump at 433 K and then it decreases up to 463 K and then increases again. Due to oxygen ion vacancy, the ac conductivity increases with the increase of frequency at the higher temperature [8]. In fact, high electric conductivity results in large leakage current for such materials in which higher dissipation present.

The dc conductivity of $\text{Bi}_{0.7}\text{Sm}_{0.3}\text{FeO}_3$ is shown in the Figure 6. It is observed that the dc-conductivity increases with increase of temperature. The activation energy has been calculated from the slope of the curve by using equation 2. The calculated activation energy (E_a) of the compound is 0.25 eV, which has been supported by previous results

[8-9]. The high value of activation energy under dc field has been obtained due to the smaller crystallite size and the higher dielectric constant.

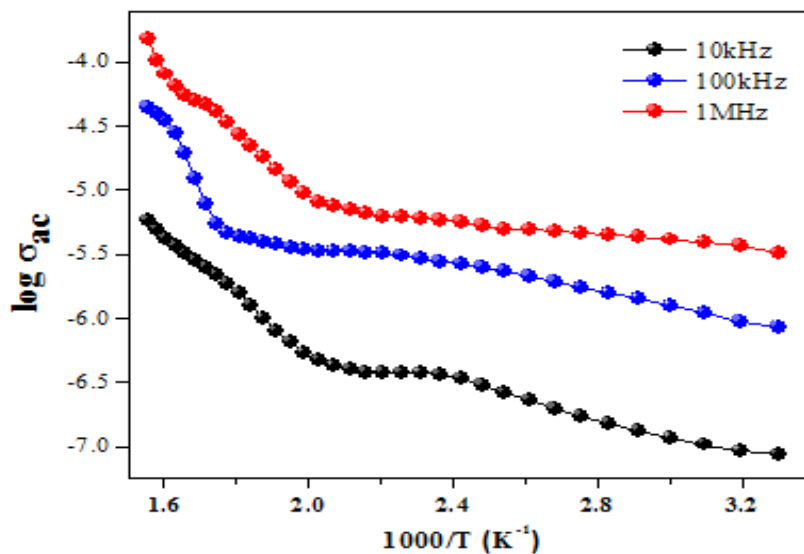


FIGURE 5. $\log \sigma_{ac}$ vs. $10^3/T$ curve

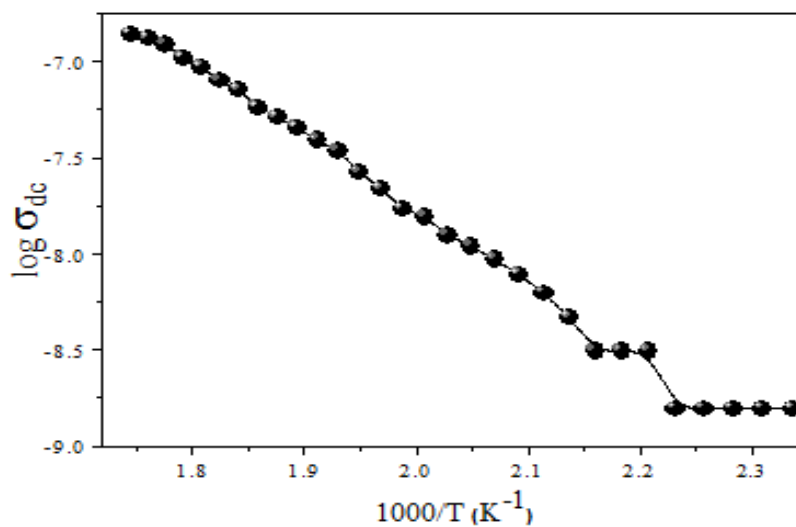


FIGURE 6. $\log \sigma_{dc}$ vs. $10^3/T$ curve

Thermal properties

Figure 7 shows the heat flow (mW) vs. temperature curve from room-temperature to 1173 K for heating cycle. The endothermic sluggish peak around 1020 K has been observed. The heat capacity (ΔC_p) and enthalpy change (ΔH) have been calculated and are 0.241 J/gK and 1.8106 J/g respectively. This low value of ΔC_p and ΔH suggests that the transition is sluggish. The weight loss vs. temperature curve is shown in the inset of Figure 7. The measured weight loss of the compound in the broad temperature range from RT to 1173 K is 0.37505 mg which is very low (1.24 % of initial weight). Here, the observed transition is so sluggish that TGA curve is unable to show appreciable weight loss near 1020K, which confirm that the material is less lossy and thermally stable.

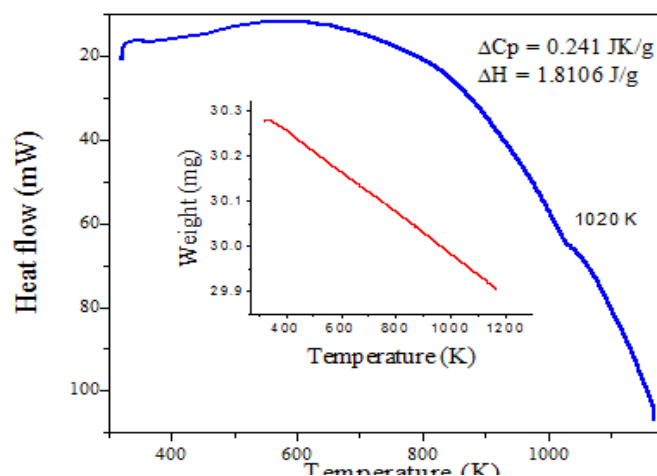


FIGURE 7. Heat Flow vs. temperature curve

CONCLUSION

Solid-state reaction method has been implemented for the preparation of $\text{Bi}_{0.7}\text{Sm}_{0.3}\text{FeO}_3$ ceramic. The compound shows orthorhombic structure with Centro-symmetric space group Pbnm. The dielectric constant and electrical conductivity studies indicate that the material reflects good dielectric behavior. The calculated activation energy (0.25 eV) under dc field compliments the smaller crystallite size and the higher dielectric characteristic of the material. The thermal property indicates that the compound is thermally stable at high temperature. High dielectric behavior along with very high thermal stability makes the compound suitable for different electronic devices.

ACKNOWLEDGMENTS

Authors are thankful to Department of Physics, MLSU Udaipur for providing XRD facility. VKJ is thankful to UGC, New Delhi for providing BSR fellowship.

REFERENCES

1. S. Jangid, S. K. Barbar, I. Bala and M. Roy, *Physica B* **407**(18), 3694-3699 (2012).
2. G. Catalan and J. F. Scott, *Nature* **448**(7156), E4-E5(2007).
3. E. M. M. Ibrahim, G. Farghal, M. M. Khalaf, H. M. A. El-Lateef, *J. Nano. Adv. Mat.* **5**(1), 33-39 (2017).
4. R. Q. Yin, B. W. Dai, P. Zheng, J. J. Zhou, W. F. Bai, F. Wen, J. X. Deng, L. Zheng, J. Du and H. B. Qin, *Ceram. Int.* **43**(8), 6467-6471 (2017).
5. T. Tong, J. Chen, D. Jin, J. Cheng, *Mater. Lett.* **197**, 160-162 (2017).
6. Z. Chen, S. Prosandeev, Z. L. Luo, W. Ren, Y. Qi, C. W. Huang, L. You, C. Gao, I. A. Kornev, T. Wu, J. Wang, P. Yang, T. Sritharan, L. Bellaiche, and L. Chen, *Phys. Rev. B* **84**, 094116 (2011).
7. Y. H. Chu, Q. Zhan, C. H. Yang, M. P. Cruz, L. W. Martin, T. Zhao, P. Yu, R. Ramesh, P. T. Joseph, I. N. Lin, W. Tian, D. G. Schlom, *Appl. Phys. Lett.* **92**, 102909 (2008).
8. Y. B. Yao, W. C. Liu, C. L. Mak, *Journal of Alloys and Compounds* **527**, 157-162 (2012).
9. E. Palaimiene, J. Macutkevicius, D. V. Karpinsky, A. L. Kholkin and J. Banys, *Applied Physics Letters* **106**, 012906 (2015).
10. A. K. Zak, W. A. Majid, M. E. Abrishami and R. Yousefi, *Solid State Science*, **13**(1), 251-256 (2011).
11. A. K. Pradhan, K. Zhang, D. Hunter, J. B. Dadson and G. B. Loutts, *J. Appl. Phys.* **97**, 093903(1-4) (2005).
12. S. A. Mir, M. Ikram and K. Asokan, *Optik* **125**, 6903-6908 (2014).
13. V. S. Puli, D. K. Pradhan, S. Gollapudi, I. Coondoo, N. Panwar, S. Adireddy, D. B. Chrisey and R. S. Katiyar, *J. Mag. & Mag. Mat.* **369**, 9-13 (2014).